Swelling of Polyelectrolyte and Polyzwitterion Brushes by Humid Vapors

Casey J. Galvin,[†] Michael D. Dimitriou,[‡] Sushil K. Satija,[‡] and Jan Genzer*,[†]

[†]Department of Chemical and Biomolecular Engineering, North Carolina State University, Raleigh, North Carolina 27695-7905, United States

[‡]NIST Center for Neutron Research National Institute of Standards and Technology, Gaithersburg, Maryland 20899, United States

S *Supporting Information*

ABSTRACT: Swelling behavior of polyelectrolyte and polyzwitterion brushes derived from poly(2-(dimethylamino)-ethyl methacrylate) (PDMAEMA) in water vapor is investigated using a combination of neutron and X-ray reflectivity and spectroscopic ellipsometry over a wide range of relative humidity (RH) levels. The extent of swelling depends strongly on the nature of the side-chain chemistry. For parent PDMAEMA, there is an apparent enrichment of water vapor at the polymer/air interface. Despite extensive swelling at high humidity level, no evidence of charge repulsion is found in weak or strong polyelectrolyte brushes. Polyzwitterionic brushes swell to a greater extent than the quaternized brushes studied. However, for RH levels beyond 70%, the polyzwitterionic brushes take up less water molecules, leading to a decline in water volume fraction from the maximum of ~0.30 down to ~0.10. Using a gradient in polymer chain grafting density (σ), we provide evidence that this behavior stems from the formation of inter- and intramolecular zwitterionic complexes.
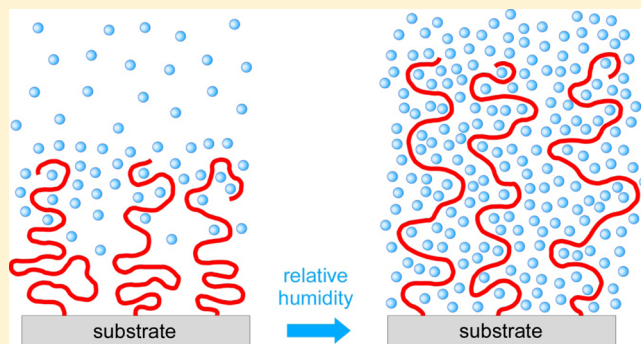
INTRODUCTION

While swelling of surface-grafted polyelectrolyte assemblies in liquids has received extensive attention,[1,2] their behavior in aqueous and organic vapors remains a largely underexplored concept. Nonetheless, the performance of these assemblies in humid and vapor-enriched environments has considerable reach, such as models for biological structures[3] or in manufacturing active layers for gas separation technologies[4] or vapor analyte sensing.[5] Swelling induced by a vapor phase is distinctly different from that by a liquid phase of the same molecule, providing new avenues of polymer physics to explore. When solvent vapors interact with a polymer film, three components must be considered, i.e., air, solvent, and polymer, compared to just solvent and polymer in the liquid phase. The interactions among these three components govern the partitioning of solvent vapor into the polymer and thus the swelling behavior of the polymer chains.

Swelling in humid environments occurs with a relatively low concentration of water in the ambient. Even at 100% relative humidity (RH), there is only ~2 wt % water present in the air at room temperature. Therefore, vapor measurements can probe the behavior of polymer brushes with low concentrations of water molecules, which are acting as solutes in a solvent of hydrophobic air. The lack of a condensed solvent phase prohibits certain phenomena observed in liquid swelling of polyelectrolyte systems, such as dissociation of counterions[6] and structuring of "liquid-like" water at a polyelectrolyte

interface.[7] The implication of these findings is that a polyelectrolyte exposed to water vapor does not necessarily act as a typical polyelectrolyte in aqueous solution. Any observed thermodynamic behavior instead results from the presence of a condensed counterion. In contrast, polysulfobe-taines, the class of polyzwitterions considered in this work, do not bear a counterion. As a result, the electrostatic charges present in the side chain can form intra- and intermolecular complexes[8,9] even without "bulk" solvent present.

Polymer brushes differ from other untethered, polymer thin film assemblies (e.g., spuncast layers) in important ways when considering swelling behavior. In the true polymer brush regime[10] for flat substrates, when the grafting density of chains (σ) is sufficiently high, polymer chains swell in the direction normal to the substrate.[2] In contrast, chains in an untethered thin film swell uniformly in all directions (except those at the substrate/polymer or polymer/air interface). Polymer brush assemblies also offer an avenue to tune σ and produce a gradient in concentration of chains in the film.[11] Controlling this parameter is not possible in untethered assemblies, which comprise a film of uniform density. Exploring the swelling behavior in polymer assemblies featuring a gradient in σ on the same sample enables one to decouple the effect of polymer crowding and RH. One can thus explore concurrently the
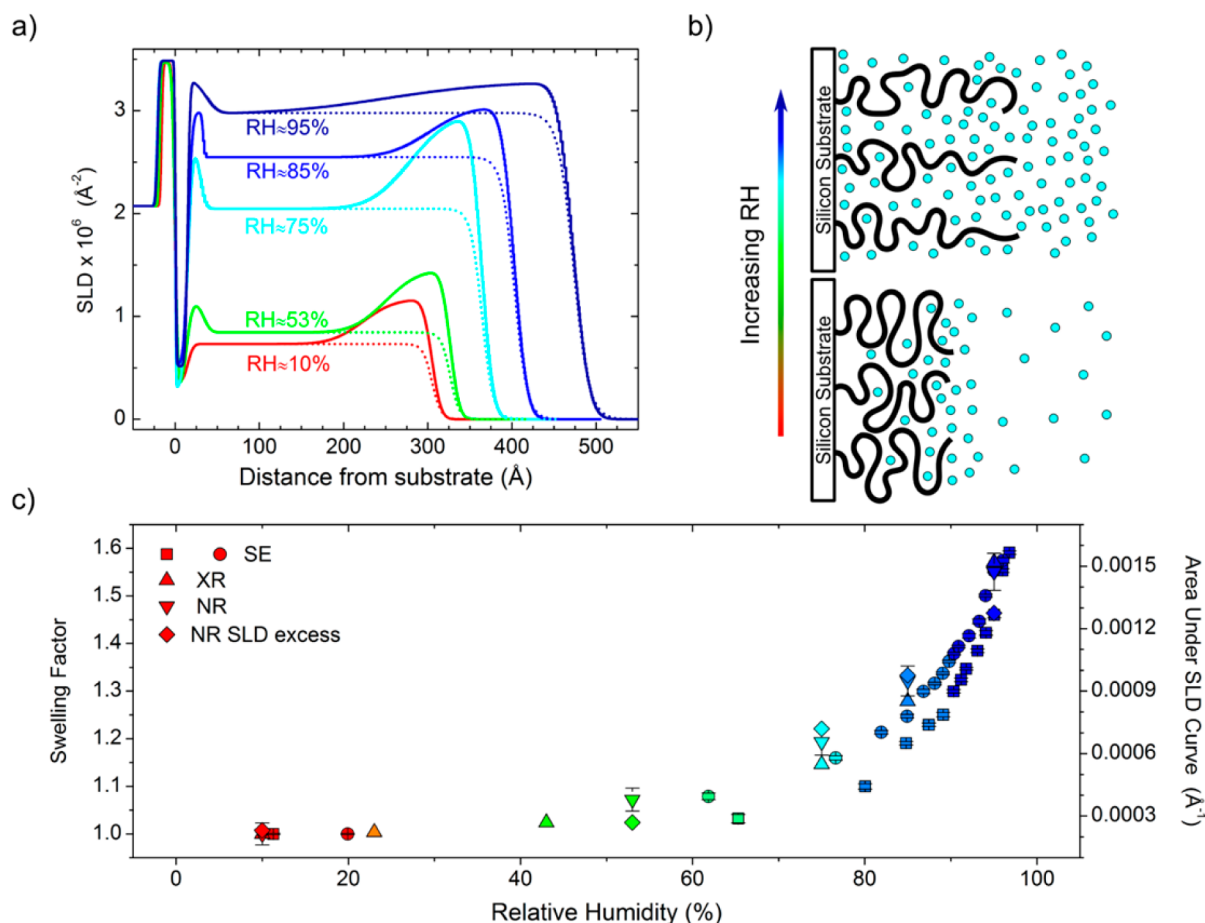
Figure 1. (a) SLD profiles at various RH levels derived from fitting NR data in Figure S1 in the SI. The colors correspond to RH level, and are consistent with those in (c). (b) Illustration of proposed D_2O enrichment at polymer/air interface at low RH (bottom), leading to more uniform hydration and chain stretching at higher RH (top). (c) Compilation of swelling factors calculated from thickness values derived from SE data (squares and circles), XR data (upward triangle) and NR data (downward triangle). The colors are consistent with (a). The right ordinate (diamonds) depicts the integrated area under the solid lines in the SLD profiles in (a).

performance of systems featuring both low and high concentration of polymer under a given RH level.

In this work we probe the swelling behavior of polyelectrolyte and polyzwitterion polymeric grafts on flat impenetrable substrates in humid environments using a combination of neutron reflectivity (NR), X-ray reflectivity (XR), and spectroscopic ellipsometry (SE). A postpolymerization modification (PPM) strategy[12,13] is employed to generate strong polyelectrolyte and polyzwitterion brushes from a weak polyelectrolyte brush "parent" of poly(2-(dimethylamino)ethyl methacrylate) (PDMAEMA). This PPM approach ensures differences in swelling behavior of the resulting samples stems from differences in side-chain chemistry. We demonstrate that, though polyelectrolytes do not experience charge repulsion, their swelling behavior depends strongly on the presence of condensed counterions and the overall hydrophobicity of the side-chain moiety. Polyzwitterion brushes exhibit a more complex swelling behavior that suggests the formation of intermolecular complexes at high σ and intramolecular complexes at low σ.

■ EXPERIMENTAL SECTION

General Methods. Acetonitrile, (dimethylamino)ethyl methacrylate (DMAEMA), methyl iodide (MeI), propyl iodide (PrI), 1,3-propane sultone (PS), dimethyl sulfoxide (DMSO), ethanol, 2,2′-bipyridyl, CuCl, and inhibitor remover packing were purchased from

Sigma-Aldrich[14] and used as received. The ATRP initiator, [11-(2-bromo-2-methyl)propionyloxy]undecyltrichlorosilane (BMPUS), was synthesized following a previously published procedure.[15] Silicon wafers (0.5 mm thick and 100 mm in diameter) were purchased from Silicon Valley Microelectronics.[14] Silicon wafers (5 mm thick and 3″ in diameter) were purchased from El-cat Inc.[14] IR spectra were collected on a Nicolet iN 10 MX microscope (Thermo Scientific[14]) in reflection mode using a liquid nitrogen cooled MCT detector with an aperture of $300~\mu m^2$ and resolution of 4 cm^{-1}.

PDMAEMA Brush Synthesis. A silicon wafer measuring 4.5 cm × 5 cm was sonicated in methanol, dried with a stream of N_2 gas, and treated in a UV−ozone chamber for 20 min. This wafer was then placed normal to a reservoir containing a 4:1 mixture of mineral oil/*n*-octyltrichlorosilane (OTS; Gelest[14]) for 7 min in an enclosed, plastic Petri dish. After OTS deposition, the wafer was immediately placed into a solution of 30 μL of 5 vol % BMPUS in anhydrous toluene and 30 mL of anhydrous toluene and incubated at −20 °C overnight. The wafer was then removed from solution, rinsed with ethanol, dried with a stream of N_2 gas, then sonicated in ethanol for 20 min and dried with a stream of N_2 gas. The wafer was then immediately analyzed by contact angle using deionized (DI) H_2O as a probing liquid and then dried with a stream of N_2 gas before immersion into a custom-built glass reactor containing the polymerization solution, which was degassed by bubbling with N_2 gas for 30 minutes while stirring. The polymerization solution comprised 50 mL of DMAEMA (purified by passing through a column containing inhibitor remover), 50 mL of DMSO, 3.1251 g 2,2′-bipyridyl, and 0.9339 g of CuCl. Following polymerization, the brush-modified wafer was rinsed with ethanol,
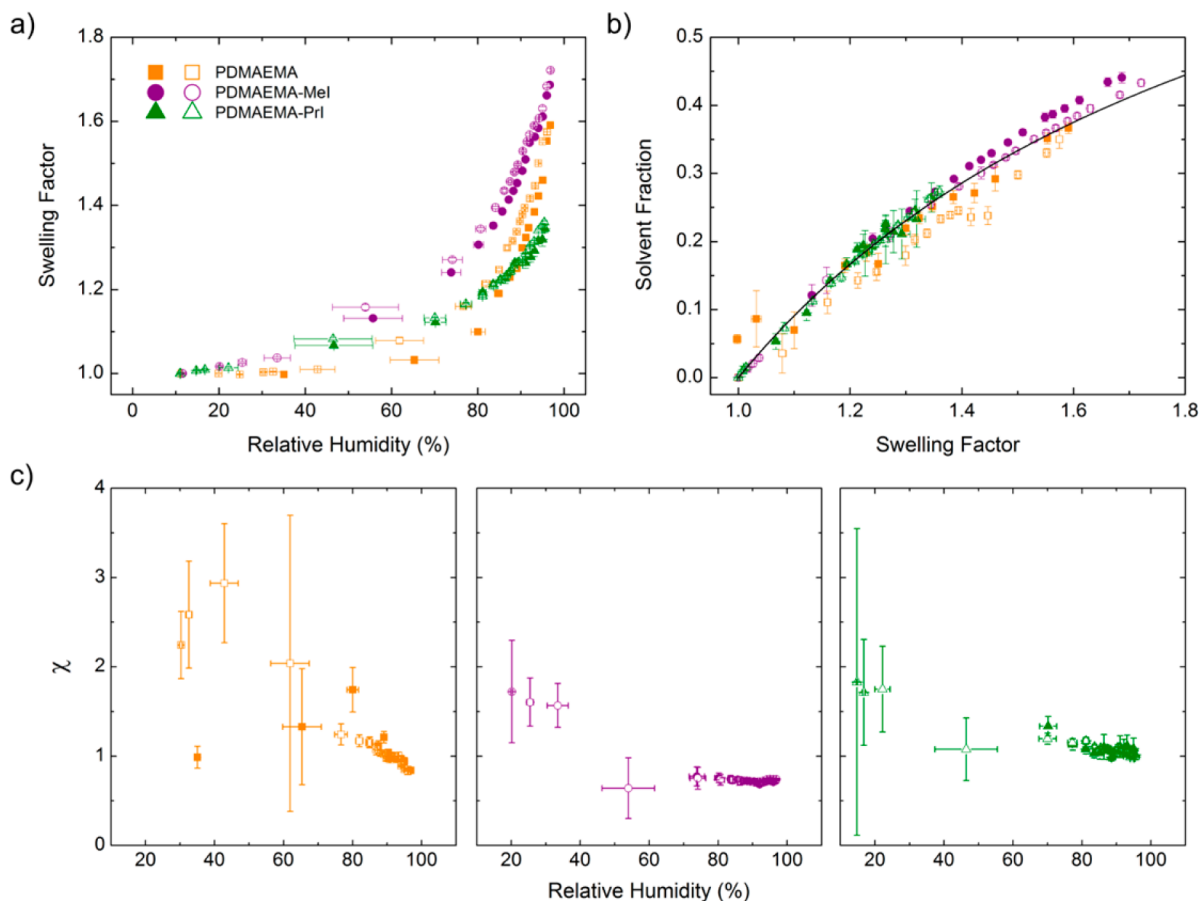
Figure 2. (a) Swelling factor for PDMAEMA (squares), PDMAEMA-MeI (circles), and PDMAEMA-PrI (triangles) calculated from thickness values derived from fitting the SE data. Closed and open symbols represent results from different runs on the same sample. (b) Solvent fraction of the polymer brush determined by fitting the SE data. Closed and open symbols represent results from different runs on the same sample. (c) Flory–Huggins χ parameter values calculated from the data in (b). Closed and open symbols correspond to results from different runs on the same sample. The error bars on the abscissa represent the range of RH levels inside the cell during a measurement for all panels.

dried with a stream of N_2 gas, then sonicated in ethanol for 20 min and dried with a stream of N_2 gas. An identical approach, without the OTS deposition step, was used to synthesize a PDMAEMA brush for reflectivity measurements on a silicon wafer (diameter 7.5 cm, thickness 5 mm). At no point in the synthesis or purification sequence was the sample exposed to liquid water.

PDMAEMA Brush Modification. The PPM reactions were carried out using 0.1 M solutions of MeI, PrI, or PS in acetonitrile at 40 °C for 48 h in an orbital shaker.[16,17] Modified samples were rinsed extensively with acetonitrile and THF, then dried under a stream of N_2 gas prior to further experiments. At no point in the modification or purification sequence were the samples exposed to liquid water.

X-ray Reflectivity. Measurements were performed using an X-ray reflectometer (Bruker, D8 Avance) employing Cu Kα radiation at National Institute of Standards and Technology (NIST) Center for Neutron Research (NCNR) (Gaithersburg, MD). The copper source was operated at 40 kV and 40 mA, and the wavelength was 0.154 nm. The beam width was 10 mm and the beam height was 0.1 mm.

Neutron Reflectivity. Measurements were performed at NG7 horizontal reflectometer at NCNR/NIST. NR was measured using a fixed wavelength of 0.475 nm and varying the incidence angle of the neutrons. During the measurement the sizes of the collimating and detector slits were increased to keep a constant footprint and a relative q resolution, $\Delta q/q$, of 0.04, where $q_z = 4\pi \sin \theta/\lambda$, and θ is the incident and final angle with respect to the surface of the film. For measurements under a humid atmosphere the sample was enclosed in an aluminum chamber with saturated salt solution source to achieve the desired humidity within the chamber.

Reflectivity Data Analysis. Reduction and analysis of the XR and NR data were done using REFLPAK suite.[18] First the off-specular scattering from the sample was subtracted from the raw data and then it was normalized against the slit scan to obtain absolute reflectivity. During a reflectivity measurement the phase information is lost so in general it is not possible to directly invert reflectivity data to real space scattering length density (SLD) profile. Instead a candidate model is assumed for the structure of the sample and then the reflectivity is calculated from this model by using optical matrix formalism. The thickness and SLD of each layer, and roughness at each interface are varied until the calculated profile agrees sufficiently well with the experimental reflectivity curve. The roughnesses between the layers are characterized using an error function.

Spectroscopic Ellipsometry. Measurements were performed on a Variable Angle Spectroscopic Ellipsometer (J.A. Woollam[14]) controlled by WVASE32 (J.A. Woollam) using a liquid cell with windows fixed at an incidence angle of 70°. Contained within the cell were two inverted vial caps (1 cm diameter) holding either pure KOH or a saturated aqueous solution of K_2SO_4. SE measurements were performed every 5 min using the Dynamic Scan feature in the WVASE32 software at an incidence angle of 70° from 400 to 1000 nm. The duration of each measurement was 3 min. A custom methacrylate lid with a single opening was used to allow access for the RH-temperature probe (Omega Engineering). The probe connected via USB to a computer that recorded temperature and RH level every 5 min at the start of each measurement. The final RH level inside the cell during a measurement was calculated as $RH_{t=0} + (3/5)*(RH_{t=1} - RH_{t=0})$, using the assumption that the increase in RH was linear over the measurement period. The approximation was found to be accurate
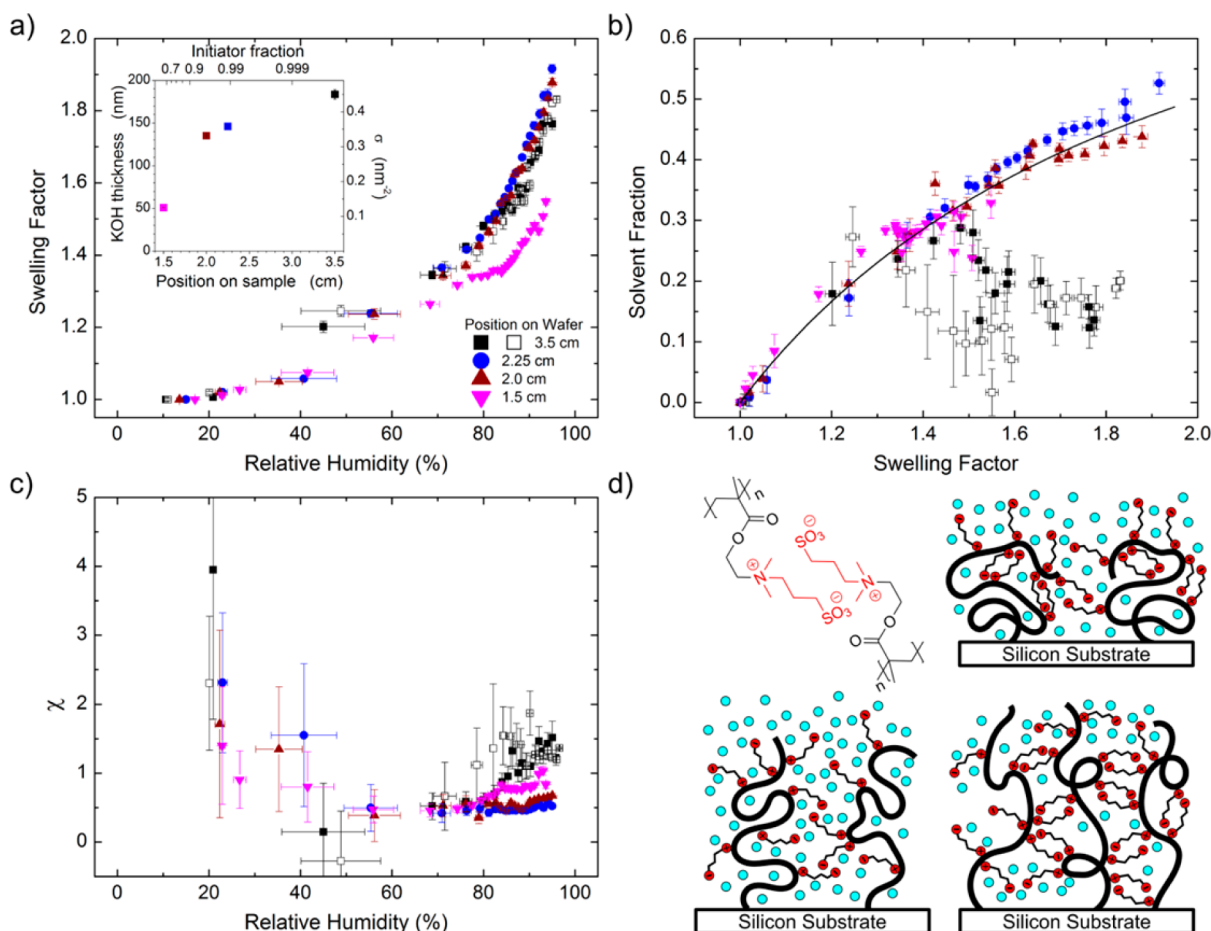
Figure 3. (a) Swelling factor values calculated from brush thicknesses obtained by fitting SE data. (Inset) Thickness of brush at ~10% RH (KOH thickness) and PDMAEMA-PS brush grafting density (σ) plotted against position on the substrate and the initiator fraction on the substrate determined by water contact angle measurements. (b) Solvent fraction inside PDMAEMA-PS brush determined by fitting SE data plotted against swelling factor values in (a). Black line is the expected trend (see text). (c) Values of Flory−Huggins interaction parameter, χ, calculated from data in (b). (d) Clockwise from upper left: illustration of zwitterion complex; low σ region forming predominantly intramolecular complexes; high σ region forming predominantly intermolecular complexes; medium σ region unable to form complexes.

within 1% RH. Note that above ~85% RH, the change in RH during a measurement is below 1%. The plots in Figures 1, 2 and 3 were constructed using the average RH level, calculated as the average of the initial and final RH levels, with the error bars showing the initial and final RH levels.

SE Data Fitting. The data collected by SE measurements at ~10% RH were fit to a model comprising a Si substrate, SiO$_x$ layer (thickness 1.5 nm) and a Cauchy layer. The Si and SiO$_x$ layers used material files supplied with the WVASE32 software. The Cauchy layer was fit using thickness, A_n and B_n. All other data at higher RH levels were fit to a similar layer, except that the polymer brush was modeled as an effective medium approximation (EMA) between the Cauchy film and H$_2$O, which used a material file supplied with the WVASE32 software. The A_n and B_n values obtained at 10% RH were used for the Cauchy film and held constant. The thickness and volume fraction of H$_2$O of the EMA were fit and used to construct plots in Figures 1, 2 and 3.

PPM Conversion Calculations. Calculations were performed as reported previously.[19] Briefly, we start from a mass balance of the polymer brush:

$$h = \frac{M_n * \sigma}{\rho * N_A} \tag{1}$$

where h is brush thickness, M_n is the number-average molecular weight of the grafted chains, σ is the grafting density of the brush, ρ is the density of the grafted chains, and N_A is Avogadro's number. Assuming a constant σ before and after brush modification (i.e., no chains

degrafting during the PPM), the conversion of the modification reaction can be estimated from the change in brush thickness. Values for molecular weight and density were taken from Sigma-Aldrich.

Reduced Grafting Density (Σ) Calculation. The grafting density (σ) of the dense brush (3.5 cm) was assumed to be 0.45 chains/nm^2 based on a prior investigation.[20] We estimated σ at the other measured points as $\sigma(x) = 0.45 * h_x / h_{3.5 \text{ cm}}$, where h_x is the thickness at the measured point at a coordinate x and $h_{3.5 \text{ cm}}$ is the thickness (90.0 nm) at 3.5 cm. The molecular weight of the high σ PDMAEMA brush was approximated as $h * 1350$ Da/nm = 90 nm * 1350 Da/nm = 121.5 kDa. The value of 1350 Da/nm stems from our assumption of $\sigma = 0.45$ chains/nm^2 and is based on prior work for polymer brushes prepared in a comparable manner.[20] That implies a degree of polymerization of ~774. Assuming the size of a monomer is 0.3 nm (calculated as $[MW_{DMAEMA}/\rho_{DMAEMA}]^{1/3}$), R_g^2 of the grafted polymer chains is ~11.6 nm^2. We then calculated $\Sigma(x) = 11.6 * \pi * \sigma(x)$ following prior work.[10]

■ RESULTS AND DISCUSSION

We employed neutron reflectivity (NR) to examine the uptake of D$_2$O vapor into a poly(2-(dimethylamino)ethyl methacrylate) (PDMAEMA) brushes grown from a silicon wafer by a surface-initiated atom-transfer radical polymerization (ATRP).[15] The RH level within the sample chamber was controlled using aqueous, saturated salt solutions (53−95% relative humidity, RH) or pure KOH (10% RH). The initial

12740

dx.doi.org/10.1021/ja5065334 | J. Am. Chem. Soc. 2014, 136, 12737−12745

PDMAEMA "KOH" thickness (i.e., thickness measured at 10% RH) was ~30 nm. Since the sample did not come into contact with liquid water at any point prior to vapor swelling measurements, the tertiary amines within the PDMAEMA brush will be neutral and not protonated. Figure 1a shows the scattering length density (SLD) profiles (solid lines) derived from fitting the reflectivity data (see Supporting Information [SI]). We identify three key features of these SLD profiles. First, as the RH level increases, the location of the polymer/air interface extends away from the substrate. There is a simultaneous increase in the SLD value of the polymer away from the substrate/polymer interface. Since D_2O has a higher SLD than the polymer layer, the data demonstrate that the PDMAEMA brush is swelling due to an uptake of D_2O vapor. From 10 to 53% RH, there is only a small change in SLD value and thickness of the film. In contrast, the SLD value and thickness both increase significantly at 75% RH, and continue to do so up to 95% RH. The second feature is a small peak present at the substrate/polymer interface for all but the lowest RH level. Since the peak indicates a region of higher SLD, there is an apparent enrichment of D_2O at the substrate/polymer brush interface.[21]

Finally, an enrichment of D_2O at the polymer/air interface exists for all RH levels. We have defined this feature as the region where the SLD profile deviates from the dotted lines indicating a constant "bulk" SLD and thus constant water level content within the brush. The shape of this peak appears similar from 10 to 75% RH. At 85% RH, the peak becomes shallower compared to the constant "bulk" SLD value, and starts to extend deeper into the brush. This trend continues to 95% RH, where the peak extends deeply into the film and is not as prominent compared to the constant "bulk" SLD value. It is noteworthy that a similar feature was not observed in NR measurements of a poly(methacrylic acid) brush in ambient humidity.[22] Furthermore, the suggested brush structure—a homogeneous "box" with a solvated interface—differs from the smooth, decreasing profile found for PDMAEMA brushes in aqueous solutions grown from silicon[23] and gold[24,25] substrates.

Figure 1b depicts pictorially the situations that resemble the partitioning of D_2O inside the PDMAEMA brushes. At low humidity levels (~10% RH), insufficient potential exists to drive D_2O vapor deep into the brush, resulting in an enrichment peak at the polymer/air interface, but no peak at the substrate/polymer interface. As more moisture is added to the air, more water molecules can sorb into and solvate the brush, leading to polymer brush swelling. That increased sorption facilitates, in turn, a deeper penetration of additional water molecules into the polymer brush, thus increasing the SLD level away from the polymer/air interface. This finding holds significant implications for the evaluation of surface properties of brushes by scanning probe techniques, which may be influenced by this enrichment.

From the data in Figure 1, it appears that at some critical RH value (~70% RH) sufficient water content exists inside the brush to swell the brush considerably, thus facilitating acceleration in moisture uptake with increasing RH. This is evident from the data plotted in Figure 1c, which depicts the swelling factor (i.e., swollen thickness normalized by thickness at 10% RH) on the ordinate determined from thickness values for the same sample using neutron and X-ray reflectivity (NR and XR, respectively). The close agreement between swelling factors derived from NR and XR measurements, the latter of which was done with H_2O, suggests that the deuterated and

hydrogenated solvents swell PDMAEMA in a similar way. The right ordinate denotes the area under the SLD profiles (solid lines) shown in Figure 1a. Both thickness and SLD profile area follow an exponential-like trend with increasing RH, confirming acceleration in moisture uptake.

Figure 1c also plots swelling factors derived from spectroscopic ellipsometry (SE) measurements for a PDMAEMA homopolymer brush ("KOH" thickness 90 nm) exposed to H_2O vapor. SE enables the simultaneous fitting of film thickness and solvent fraction (ϕ), making it a practical substitute for reflectivity measurements. We performed SE measurements while ramping RH levels inside an enclosed sample chamber fitted with a probe capable of recording concurrently temperature and RH. The humidity was adjusted using either dry KOH or saturated aqueous solutions of K_2SO_4. Prior work using a similar technique found that the swelling of a polymer film corresponded precisely with changes in RH.[26] We found that KOH attains an equilibrium RH level of ~10% in our chamber, while K_2SO_4 reaches ~96%. Since we measure the RH level inside the chamber, we can track the response of the polymer brushes to the changing environment during equilibration. We are thus not limited to the equilibrium RH value of the saturated salt solution. All measurements were performed at ambient lab temperature of 23.5 ± 0.5 °C. We deliberately maintained the RH level below 96% to ensure no condensation occurred within the chamber. The comparable results obtained between the different experimental techniques serve to confirm our experimental observations, as well as validating the use of SE in analyzing polymer brush swelling in humid environments.

Using a postpolymerization modification (PPM) strategy,[12] we synthesized a series of polymer brushes derived from the same PDMAEMA homopolymer parent brush. By using samples from this parent polymer brush, we can ensure similar degrees of polymerization (DP) and grafting densities (σ) between samples, assuming no chains are cleaved from the substrate during the PPM reaction. The resulting sample library consists of the neat PDMAEMA, two quaternized samples with a methyl (PDMAEMA-MeI) or propyl (PDMAEMA-PrI) alkyl chain and iodide counterions, and a sample betainized with PS (PDMAEMA-PS), producing a polyzwitterion. These side-chain chemistries are depicted in Scheme 1. Note that betainization does not produce a counterion, instead yielding unshielded charges. This library provides a means to study systematically the effect of introducing permanent charges, hydrophobic moieties, and zwitterions into the polymer side chain on swelling in humid environments. By monitoring how these materials swell over a wide, smoothly varying range of RH levels, we illustrate how side-chain chemistry influences the sorption behavior of water vapor.

Thicknesses of the initial and modified samples at low RH (~10%, termed "KOH" thickness) are listed in Table 1, along with an estimated conversion based on a mass balance using a methodology reported previously.[19] This conversion estimate provides an upper limit, as there is likely still some residual moisture in these brushes even at 10% RH. Characterization of the samples with infrared spectroscopy suggests a quantitative conversion of the tertiary amine to the respective modified structures (see SI), which is consistent with the calculations for PDMAEMA-MeI and PDMAEMA-PrI. The refractive indices of the modified films increase relative to the unmodified PDMAEMA brush (see SI), suggesting that solvent does not remain trapped inside of the film. Calculations for PDMAEMA-

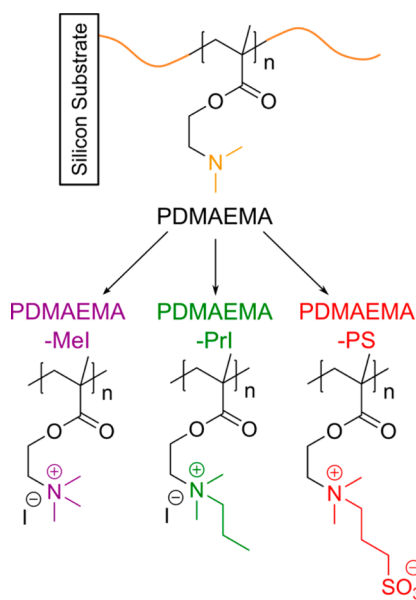**Scheme 1. Polyelectrolyte and Polyzwitterion Brushes Derived from PPM Reactions**

Table 1. Selected Properties of Polymer Brush Samples Prepared by PPM

sample name	"KOH" thickness (nm)	thickness after PPM/"KOH" thickness	implied conversion
PDMAEMA	90.0 ± 0.2	N/A	N/A
PDMAEMA-MeI	122.9 ± 0.1	1.37	0.99
PDMAEMA-PrI	138.2 ± 1.0	1.54	0.97
PDMAEMA-PS	183.0 ± 5.6	2.03	1.4 (see text)

PS predict a conversion greater than 100%, which, we believe, results from an incorrect assumption that the density of the modified polymer represents a weighted average of the density of PDMAEMA and the PS modifying agent. Our measurements imply that the density of the modified repeat unit is closer to 0.8 g/cm^3, compared to an anticipated value of 1.09 g/cm^3 (see SI). This lower density would lead to a thicker brush at a given modification, and possibly stems from charge repulsion due to the unshielded charges present in PDMAEMA-PS. While the repeat units of modified PDMAEMA-PS are overall neutral, the very tip of the side chain bears an anionic sulfonate group. Repulsion between sulfonate groups would lead to stretching of the brush even in air. Since the quaternized samples bear condensed counterions that shield neighboring charges, no repulsion is present in air. As a result, the quaternized samples behave like uncharged systems in air, and their modified thickness is well-predicted by a mass balance.

Figure 2a plots the swelling factor of the unmodified and quaternized samples versus the average RH level over the duration of the SE measurement for two measurements of the same sample. Note that the PDMAEMA data are the same as in Figure 1. We observe a strong influence of side-chain chemistry of the modified samples on the extent of swelling. Of the three samples, PDMAEMA-MeI exhibits the largest extent of swelling over the entire measurement range. While PDMAEMA exhibits initially the least swelling, the polymer brush swells rapidly at RH > 75%. Overall, PDMAEMA-PrI swells more than PDMAEMA at lower RH levels, but much less than PDMAEMA at higher RH levels. The data in Figure 2b

illustrate the relationship between solvent fraction and swelling factor derived from the SE data. PDMAEMA, PDMAEMA-MeI, and PDMAEMA-PrI follow the expected relationship, $\phi = 1 - 1/$swelling factor (black line in Figure 2b). From this trend we conclude that the swelling observed in the data in Figure 2a is due to uptake of water, since increasing thickness is correlated, as expected, with increasing ϕ. This finding implies that charge repulsion is not contributing to the swelling process, in line with prior observations.[6] These results illustrate the interplay between the ammonium salt of the quaternized samples and the relative length of the attached alkyl chain. Through ~50% RH, the presence of the ammonium salt leads to an increased uptake of water in the quaternized samples compared to PDMAEMA. Eventually, the quaternized samples deviate from one another, and PDMAEMA-MeI swells appreciably more than PDMAEMA-PrI due to the difference in hydrophobicity between the methyl and propyl group. The onset of this deviation may occur when most of the available sites near the condensed counterion are occupied by water molecules.

Further insight can be gained by analyzing these data in the context of Flory−Huggins theory. We calculated the interaction parameter, χ, as[27]

$$\chi = \frac{\ln\left(\frac{RH/100}{\phi}\right) + \phi - 1}{(1 - \phi)^2} \qquad (2)$$

and plotted the resultant values of χ in Figure 2c. The large error bars at lower RH levels stem from the large relative error associated with ϕ values. For example, $\phi = 0.02 \pm 0.01$ is a small amount of moisture overall, but represents 50% error; propagating this error to a value on the order of 2 leads to error bars of ±1. At higher RH levels, ϕ values are larger, while error values remain about the same on an absolute basis, resulting in significantly lower relative error. We note this issue as a limitation of SE measurements on these types of samples. Nonetheless, data at lower RH levels reveal a notable trend. Regardless of the side-chain chemistry, all the samples have higher χ values at lower RH levels. Recalling that air is a hydrophobic medium, we reason that the polymer chains have arranged themselves to minimize exposure of any hydrophilic groups with the air. Interestingly, PDMAEMA-MeI and PDMAEMA-PrI both have χ values in the range of 1.5−1.75 at ~20% RH, while PDMAEMA is ~2.5. This difference may stem from the presence of the ammonium salt. Since the two quaternized samples have comparable values, the length of the alkyl chains studied here may not contribute meaningfully at these RH levels.

The trends in χ at higher RH levels reveal that PDMAEMA grows increasingly hydrophilic with increasing RH, with χ moving from ~1.25 to 0.85, confirming a result found for solvent-cast PDMAEMA films.[28] This decreasing χ value suggests that the polymer grafts are being solvated by the present water molecules, providing a mechanism for the observations seen in Figure 1. As the enrichment zone extends deeper into the brush, the overall χ value for the polymer film decreases, as seen in the data in Figure 2. The quaternized samples, PDMAEMA-MeI and PDMAEMA-PrI, exhibit χ values of ~0.7 and ~1.05, respectively, which remain constant within error. These χ values quantify the effect of the more hydrophobic propyl chain in PDMAEMA-PrI relative to the methyl moieties present in PDMAEMA-MeI. Furthermore, the

fact that these χ values are constant suggests that these films are not hydrated in the same way as the unmodified PDMAEMA.

Recent work in developing advanced vapor sensors demonstrated an improved sensitivity in sensors that employed brush architectures as the sensing layer compared to a drop cast film of the same polymer.[5] The behavior of the unmodified and quaternized brushes in Figure 2 illustrate that the chemistry of the film also can substantially affect the film response. In this case, the PDMAEMA-MeI brush shows increased sensitivity to the ambient RH level relative to the PDMAEMA and PDMAEMA-PrI brushes. Furthermore, quaternization leads to a more uniform and predictable swelling response of the brush to RH level, evidenced by the uniform χ value for PDMAEMA-MeI and PDMAEMA-PrI above ~50% RH. This combination of chemistry and architecture may be a platform for innovation as surface-grafted polymer assemblies move from nanoscience to nanotechnology. A PPM synthesis strategy provides a straightforward way to leverage this combination.

Finally, we consider the behavior of the polyzwitterion sample, which comprised a gradient in σ of polymer assemblies prepared using a strategy developed earlier.[11] Figure 3a plots the swelling factor for points measured along the gradient. The legend names indicate the distance of the measured point from the silane reservoir used in the gradient deposition, such that 0 cm indicates the end of the silicon wafer immediately adjacent to the reservoir. Note that the unmodified and quaternized samples described above were taken from the homogeneous portion of the same σ gradient sample. The sample at 3.5 cm is the PDMAEMA-PS specimen described in Table 1. The inset shows the "KOH" thickness of the samples (left ordinate) as a function of position on the sample (lower abscissa) and initiator fraction (upper abscissa) as determined from water contact angle measurements prior to polymerization. As one moves along the wafer from position 1.5 cm to position 3.5 cm, the initiator fraction increases. Assuming that no significant variation in M_n occurs within the sample, the change in thickness with initiator fraction results from extension of the chains away from the substrate/polymer interface due to increased σ. By assuming $\sigma = 0.45$ chains/nm^2 for the thickest region of the brush,[20] we estimate the σ values for the other regions of the brush (right ordinate in the inset to Figure 3a). In the discussion that follows we will refer to the brush at 3.5 cm as "high σ" (~0.45 chains/nm^2), at 2.25 and 2.0 cm as "medium σ" (~0.35 chains/nm^2), and at 1.5 cm as "low σ" (~0.13 chains/nm^2). The term "brush" is used for simplicity, even if the grafted assembly may not be in a true brush regime.

Compared to the unmodified and quaternized samples, the high and medium σ regions of PDMAEMA-PS swell to the greatest extent. The high and medium σ regions show similar swelling factors, while the low σ region swells considerably less. Note that PDMAEMA-PS showed the greatest extent of stretching after modification, and also swells smoothly to the greatest extent at the highest RH levels for high and medium σ. These findings suggest that stretching induced by modification reactions prior to vapor swelling measurements does not affect the swelling behavior for the σ and MW values considered here. Employing samples that express an additional MW gradient[29] over a wide parameter space—particularly higher MW values (i.e., thicker films)—would provide better insight into the conditions which show a plateau in swelling behavior.

The extent of interaction between neighboring chains can be described using reduced grafting density (Σ), defined as $\Sigma = \sigma \pi R_g^2$, where R_g is the radius of gyration of the polymer chain.

Based on values for the unmodified PDMAEMA gradient, this measurement point has a value Σ of ~5.6 (see Experimental Section for calculation), suggesting the low σ region is in the weakly interacting regime.[10] In contrast, the medium and high σ regions have Σ values of ~13.6 and ~16.4, respectively, placing them very close to or in the brush regime. Since the low σ chains are less confined, they are able to swell laterally to a certain extent. In contrast, the chains at the high and medium σ regions swell primarily in the direction normal to the substrate. As a result, these regions have a higher swelling factor. For the measurements at 1.5 cm, there is an apparent shift in trend at 75 RH %. We hypothesize that the origin of this feature is related to a change in the brush's regime as a result of increased interactions between chains due to swelling.

Figure 3b plots the same relationship between ϕ and swelling factor as in Figure 2b. While the high and medium σ regions exhibit similar swelling behavior, their uptake of solvent differs markedly. The medium σ region follows the expected trend (solid black line), confirming that the increased thickness is due to an uptake of H$_2$O vapor. In contrast, the data for the high σ brush deviate markedly from this trend at a swelling factor of ~1.4 (~75% RH). The low σ region follows the expected relationship for ϕ. For comparison, recall that the unmodified and quaternized samples, which have comparable σ, follow this trend. We conclude that the shift in trend for PDMAEMA-PS at high σ density is due to sufficient proximity between chains to enable interactions between the unshielded charges in the brush side chains.

The expected trend plotted in Figure 2b and Figure 3b assumes a constant polymer density throughout the swelling process (i.e., the solvent and polymer volumes are additive). In order for PDMAEMA-PS to continue swelling while maintaining a constant H$_2$O volume fraction, the volume of polymer in the system must change to compensate for the increased volume of water vapor in the film. Since only PDMAEMA-PS exhibits this behavior, we conclude that the presence of opposite, unshielded charges (i.e., no counterions) accounts for our observations. Specifically, the anionic charge of one side chain can interact with the cationic charge of a nearby side chain, and vice versa.[30] The resulting complexes will possess an overall higher density, since two interacting side chains will occupy less volume than two noninteracting or repulsive side chains. On the basis of a mass balance, increasing the polymer density would actually lead to a reduction in film thickness (see PPM Conversion Calculations in the Experimental Section). Therefore, in order for complexes to form while the brush continues to swell, these complexes are able to break and reform dynamically in response to forces induced by increasing osmotic pressure from increased vapor in the brush.

This dynamic formation of zwitterion complexes may explain the trend in ϕ for the high σ region. Perhaps as the high σ region of the brush swells, the zwitterion complexes will start to resemble a ladder-like structure. Incremental addition of a water molecule into the brush may lead to reorganization of the complexes near the added water molecule that propagates along the chain, resulting in a long-range rearrangement of the chain. This rearrangement might lead to a relatively large increase in swelling factor since the rearrangement occurs over a long distance, while leading to an overall reduction in ϕ since a relatively small amount of water induced the change in swelling factor.

Figure 3c plots the χ parameter for the PDMAEMA-PS gradient. As before, we observe higher χ values at lower RH

levels, consistent with the idea that hydrophobic moieties are preferentially exposed to the air. At higher RH levels, the samples converge to a χ value of 0.5 near 70 RH %. With increasing RH, the regions of highest and lowest σ show an increasing χ parameter, while the medium σ regions remain essentially constant at 0.5. An increasing χ value implies the brush is becoming more hydrophobic, and has been observed in thin films of PDMAEMA-PS.[31] Complexing within PDMAE-MA-PS will compensate the charges in the zwitterion, reducing the interaction with water vapor,[32] and resulting in a relatively hydrophobic environment comprising propyl spacers and hydrocarbon backbones. It appears that intermolecular zwitterion complexes form at the highest σ. In contrast, the increase in χ value at the lowest σ may stem from intramolecular zwitterion complexes. Between these two extremes, polymer chains at medium σ do not appear to form significant complexes because the solvent fraction follows the expected dependence on the swelling factor. Likely, polymer grafts at these locations on the substrate do not have high enough σ to form intermolecular complexes, but are too dense to allow the chain to coil back on itself and form intramolecular complexes. This scenario is illustrated in Figure 3d.

The reason humidity can induce the formation of these complexes is not completely clear from our data. One possibility is that the moisture solvates the polymer chains, affording the betaine moieties enough mobility to form complexes. Below a critical humidity level, the system has insufficient mobility to do so. The moisture may also screen repulsion between neighboring sulfonate groups, lowering the energy barrier for a complex to form. Regardless of the mechanism by which these complexes form, our findings illustrate the significant differences in physical behavior that can result from processing conditions of the underlying brush. Care must be taken to account for differences in brush parameters like σ when comparing across experimental results.[10] Moreover, this dependence of the PDMAEMA-PS swelling behavior on σ illustrates another tunable parameter for technologies employing surface-grafted polymer assemblies. As these grafted assemblies find broader use, it is worth noting that multiple parameters (e.g., σ and side-chain chemistry) determine their physical behavior, and that the desired behavior may occur at an intermediate value of these multiple parameters. The use of gradient samples proves invaluable in this regard, since they provide an internal reference and smooth variation in parameter space.

CONCLUSION

We have demonstrated the strong influence that side-chain chemistry has on the swelling of polyelectrolyte and polyzwitterion brushes. Weak polyelectrolyte brushes of PDMAEMA are hydrated heterogeneously due to solvation of the polymer/air interface. While incorporating a condensed counterion into a polymer brush through quaternization tends to increase moisture uptake at lower humidity levels, the hydrophobicity of the modified side chain can result in overall less swelling compared to the unmodified polymer brush. Compared to unmodified PDMAEMA, quaternized brushes exhibit a more uniform swelling response to increasing humidity levels. Furthermore, charge repulsion does not influence film swelling due to the presence of a condensed counterion. In contrast, incorporation of zwitterion chemistry into the side chain produces complex moisture uptake behavior.

The extent of moisture uptake appears to depend on the extent of zwitterion complex formation, which can occur as both intermolecular and intramolecular interactions depend on the grafting density of the polyzwitterion brush. The implication from our results is that the most hydrophilic polysulfobetaine brush occurs at an intermediate grafting density that minimizes the formation of these complexes. These findings point to a means to tailor the response of surface-grafted polymer assemblies for vapor sensing, gas separations, and other technologies.

ASSOCIATED CONTENT

Supporting Information
Neutron reflectivity curves, predicted swelling factors from the modification reactions, and FT-IR spectra and refractive indices of the polymer brush samples. This material is available free of charge via the Internet at http://pubs.acs.org.

AUTHOR INFORMATION

Corresponding Author
jan_genzer@ncsu.edu

Notes
The authors declare no competing financial interest.

REFERENCES

(1) Rühe, J.; Ballauff, M.; Biesalski, M.; Dziezok, P.; Gröhn, F. D; Rühe, J. *Adv. Polym. Sci.* **2004**, *165*, 79−150.
(2) Toomey, R.; Tirrell, M. *Annu. Rev. Phys. Chem.* **2008**, *59*, 493−517.
(3) Button, B.; Cai, L.-H.; Ehre, C.; Kesimer, M.; Hill, D. B.; Sheehan, J. K.; Boucher, R. C.; Rubinstein, M. *Science* **2012**, *337*, 937−941.
(4) Grajales, S. T.; Dong, X.; Zheng, Y.; Baker, G. L.; Bruening, M. L. *Chem. Mater.* **2010**, *22*, 4026−4033.
(5) McCaig, H. C.; Myers, E.; Lewis, N. S.; Roukes, M. L. *Nano Lett.* **2014**, *14*, 3728−3732.
(6) Biesalski, M.; Rühe, J. *Langmuir* **2000**, *16*, 1943−1950.
(7) Uosaki, K.; Noguchi, H.; Yamamoto, R.; Nihonyanagi, S. *J. Am. Chem. Soc.* **2010**, *132*, 17271−17276.
(8) Bredas, J.; Chance, R.; Silbey, R. *Macromolecules* **1988**, *21*, 1633−1639.
(9) Schlenoff, J. B. *Langmuir* **2014**, *30*, 9625−9636.
(10) Brittain, W. J.; Minko, S. *J. Polym. Sci. Part A Polym. Chem.* **2007**, *45*, 3505−3512.
(11) Wu, T.; Efimenko, K.; Genzer, J. *J. Am. Chem. Soc.* **2002**, *124*, 9394−9395.
(12) Galvin, C. J.; Genzer, J. *Prog. Polym. Sci.* **2012**, *37*, 871−906.
(13) Günay, K. A.; Theato, P.; Klok, H.-A. *J. Polym. Sci., Part A: Polym. Chem.* **2013**, *51*, 1−28.
(14) Commercial materials, instruments and equipment are identified in this paper to specify the experimental procedure as completely as possible. In no case does such identification imply a recommendation or endorsement by the National Institute of Standards and Technology nor does it imply that the materials, instruments, or equipment identified are necessarily the best available for the purpose.
(15) Matyjaszewski, K.; Miller, P. J.; Shukla, N.; Immaraporn, B.; Gelman, A.; Luokala, B. B.; Siclovan, T. M.; Kickelbick, G.; Vallant, T.; Hoffmann, H.; Pakula, T. *Macromolecules* **1999**, *32*, 8716−8724.
(16) Jaeger, W.; Bohrisch, J.; Laschewsky, A. *Prog. Polym. Sci.* **2010**, *35*, 511−577.
(17) Lowe, A. B.; McCormick, C. L. *Chem. Rev.* **2002**, *102*, 4177−4190.

(18) Kienzle, P. A.; O'Donovan, K. V.; Ankner, J. F.; Berk, N. F.; Majkrzak, C. F. http://www.ncnr.nist.gov/reflpak/.

(19) Arifuzzaman, S.; Ozçam, A. E.; Efimenko, K.; Fischer, D. A.; Genzer, J. *Biointerphases* **2009**, *4*, FA33−44.

(20) Tomlinson, M. R.; Genzer, J. *Langmuir* **2005**, *21*, 11552−11555.

(21) Vogt, B. D.; Soles, C. L.; Jones, R. L.; Wang, C.-Y.; Lin, E. K.; Wu, W.; Satija, S. K.; Goldfarb, D. L.; Angelopoulos, M. *Langmuir* **2004**, *20*, 5285−5290.

(22) Deodhar, C.; Soto-Cantu, E.; Uhrig, D.; Bonnesen, P.; Lokitz, B. S.; Ankner, J. F.; Kilbey, S. M. *ACS Macro Lett.* **2013**, *2*, 398−402.

(23) Sanjuan, S.; Perrin, P.; Pantoustier, N.; Tran, Y. *Langmuir* **2007**, *23*, 5769−5778.

(24) Jia, H.; Wildes, A.; Titmuss, S. *Macromolecules* **2012**, *45*, 305−312.

(25) Rauch, S.; Uhlmann, P.; Eichhorn, K.-J. *Anal. Bioanal. Chem.* **2013**, *405*, 9061−9069.

(26) Mukherjee, M.; Souheib Chebil, M.; Delorme, N.; Gibaud, A. *Polymer (Guildf).* **2013**, *54*, 4669−4674.

(27) Flory, P. J. *Principles of Polymer Chemistry*; Cornell University Press: Ithaca, NY, 1953; p 672.

(28) Arce, A.; Fornasiero, F.; Rodriguez, O.; Radke, C. J.; Prausnitz, J. M. *Phys. Chem. Chem. Phys.* **2004**, *6*, 103−108.

(29) Tomlinson, M. R.; Genzer, J. *Macromolecules* **2003**, *36*, 3449−3451.

(30) Cheng, N.; Brown, A. A.; Azzaroni, O.; Huck, W. T. S. *Macromolecules* **2008**, *41*, 6317−6321.

(31) Galin, J.; Galin, M. *J. Polym. Sci., Part B: Polym. Phys.* **1992**, *30*, 1113−1121.

(32) Kondo, T.; Nomura, K.; Murou, M.; Gemmei-Ide, M.; Kitano, H.; Noguchi, H.; Uosaki, K.; Ohno, K.; Saruwatari, Y. *Colloids Surf., B* **2012**, *100*, 126−132.